

# Analytical and numerical studies of quantization effects in coherent optical OFDM transmission with 100 Gbit/s and beyond

Michael Bernhard, David Rörich, Thomas Handte, Joachim Speidel

Universität Stuttgart, Institut für Nachrichtenübertragung  
{bernhard, roerich, handte, speidel}@inue.uni-stuttgart.de

## Abstract

For the implementation of real-time optical orthogonal frequency division multiplexing (O-OFDM) systems at data rates of 100 Gbit/s and beyond, quantization effects due to the limited resolutions of digital-to-analog converter (DAC) and analog-to-digital converter (ADC) play an important role. We study these effects both analytically and by simulation and present methods to mitigate their impact on signal quality and channel estimation.

## 1 Introduction

Several experiments have shown that O-OFDM is a promising modulation technique for optical communications. Also real-time experiments have been carried out using a field programmable gate array (FPGA) with data rates of up to 24 Gbit/s [1], [2], [3], [4]. Next step on the way to data rates of 100 Gbit/s and more is the development of an integrated circuit (IC) of an OFDM transmitter [5] that also includes the DAC.

### 1.1 Overview of system model

The system model shown in **Fig. 1** has been used for numerical simulations. It consists of an OFDM transmitter, an optical link and an OFDM receiver. At the transmitter side, the data signal from a random bit source is parallelized in the electrical domain. The following OFDM transmitter consists of a mapper (MAP), an inverse fast Fourier transform (IFFT), a guard interval inserter (GI) and a serializer (P/S). For the IFFT, we use an idealized model with double precision and a hardware model written in Very High Speed Hardware Description Language (VHDL) which takes limited word lengths into account. A requantizer unit (Requant) connects the OFDM transmitter to the DAC. This unit is required to adapt different word lengths of OFDM transmitter output and DAC input. Two DACs are required, one for the in-phase and one for the quadrature component. The optical transmit signal is generated by an external optical modulator and a laser diode. The optical link consists of a standard single mode fiber (SSMF) with a length of 80 km. Major impairments to the optical signal are chromatic dispersion and attenuation of the fiber. On the receiver side, the signal is amplified by an erbium doped fiber amplifier (EDFA) and a 90°-hybrid converts the optical signal into an analog electrical signal which is fed to two ADCs. The OFDM receiver parallelizes (S/P) the incoming data, then the guard interval is removed

(GI<sup>-1</sup>). The fast Fourier transform (FFT) converts the signal from time domain to frequency domain and is followed by an equalizer (EQ). After demapping (DEMAP) the signal is serialized and a bit error measurement can be arranged. The mapper can be chosen to

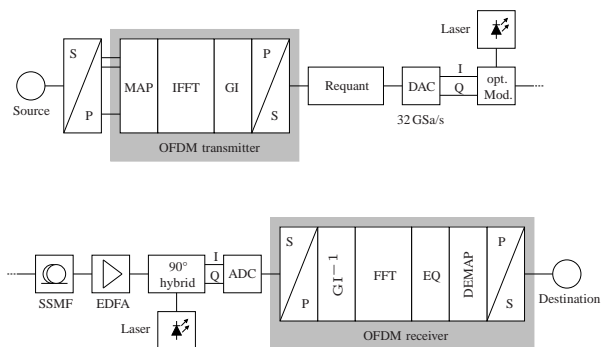


**Figure 1** System model of O-OFDM transmission.

generate 4-, 16- or 64-quadrature amplitude modulation (QAM) symbols. The amount of zero padded subcarriers is one third of the total number of subcarriers. The IFFT size is 256 and in the hardware model its output word length is 14 bit. The guard interval consists of 8 samples and is implemented as cyclic pre- and postfix. The DAC operates with 32 GSa/s and its input word length can be adjusted in the range from 4 bit up to 8 bit. The ADC operates with a sampling frequency of 32 GSa/s. We can also vary the output word length of the ADC. Furthermore, it is possible to bypass DAC and ADC without quantization. The equalizer is implemented as a one tap filter in the frequency domain with data-aided channel estimation that is explained in Section 5 in more detail. The envisaged data rates shall be achieved using polarization multiplex with 80 Gbit/s using 4-QAM, 160 Gbit/s using 16-QAM and up to 240 Gbit/s using 64-QAM. In this model, we do not consider polarization mode dispersion (PMD) and assume that it is perfectly equalized.

In this paper we start with an analytical model of quantization and clipping noise and verify it with numerical simulations in Section 2. Then we present a hardware solution for requantization with low complexity in Section 3 and show the impact on the system performance. In Section 4 we study a reduced input word length of the ADC and its effects and in Section 5 the influence of requantization on channel estimation is shown including some proposals to improve the system performance. Finally, Section 6 concludes the most important results.

## 2 Analytical model of quantization and clipping noise

The real or imaginary part  $x(t)$  of a time domain OFDM signal with mean power  $\mathbb{E}[x^2] = \sigma^2$  can be well approximated by a Gaussian random process with zero mean [6]. It becomes apparent from this fact that high peaks are rare events compared to low amplitude levels. The output signal of the DAC is represented by a limited number of  $2^M$  discrete values and therefore incorporates quantization noise. On transmitter side,  $M$  is determined by the DAC resolution. To reach bit rates of 100 Gbit/s and more DAC and ADC have to be operated at extremely high speeds (greater than 30 GSa/s) where the achievable effective number of bits does not exceed 6 bit/sample at the moment [7], [8], [9]. Combined with high peak-to-average power ratio (PAPR) this leads to significant quantization impairments, especially for higher modulation orders as will be shown in Section 3. To reduce quantization noise, the PAPR of the signal can be limited by clipping the signal amplitude. However, as the clipping process introduces additional noise, a trade-off between clipping and quantization noise has to be found. In the following we derive an expression for the signal-to-noise ratio (SNR) after clipping and quantization along the lines presented by Mestdagh et al. [10] that will allow us to determine the optimal clipping ratio for a given ADC/DAC resolution. The probability density function of the signal amplitude  $x$  is given by

$$p(x) = \frac{1}{\sigma\sqrt{2\pi}} e^{-\frac{x^2}{2\sigma^2}} \quad (1)$$

and the clipped signal is defined by

$$\tilde{x}(t) = \begin{cases} x(t) & |x(t)| < C \\ C & |x(t)| \geq C \end{cases}, \quad (2)$$

where  $C > 0$  is the clipping threshold. The average power of the clipping noise  $x(t) - \tilde{x}(t)$  can be calculated by

$$N_{\text{clip}} = 2 \int_C^\infty (x - C)^2 p(x) dx \quad (3)$$

from which we obtain using (1)

$$N_{\text{clip}} = 2(\sigma^2 + C^2) Q\left(\frac{C}{\sigma}\right) - 2C \frac{\sigma}{\sqrt{2\pi}} e^{-\frac{C^2}{2\sigma^2}}, \quad (4)$$

where  $Q(z) = (1/\sqrt{2\pi}) \int_z^\infty \exp(-u^2/2) du$  denotes the Q-function. After clipping, the signal will be quantized with  $2^M$  equidistant discrete values. The quantization interval  $q$  is thus

$$q = \frac{2C}{2^M} \quad (5)$$

and under the assumption of a uniformly distributed quantization error, which has been shown to be an accurate approximation [11], we obtain the mean quantization noise power

$$N_q = \frac{q^2}{12} = \frac{C^2}{3 \cdot 2^{2M}}. \quad (6)$$

Assuming that clipping and quantization noise are statistically independent, summation of (4) and (6) yields the total noise power. Then, the SNR  $\gamma$  follows as

$$\begin{aligned} \gamma &= \frac{\sigma^2}{N_{\text{clip}} + N_q} \\ &= \left[ 2(1 + \zeta) Q(\sqrt{\zeta}) - \sqrt{\frac{2\zeta}{\pi}} e^{-\frac{1}{2}\zeta} + \frac{\zeta}{3 \cdot 2^{2M}} \right]^{-1}. \end{aligned} \quad (7)$$

In (7) we introduced the clipping ratio  $\zeta$  defined as  $\zeta = C^2/\sigma^2$ . **Fig. 2** shows  $\gamma$  as a function of  $\zeta$  and

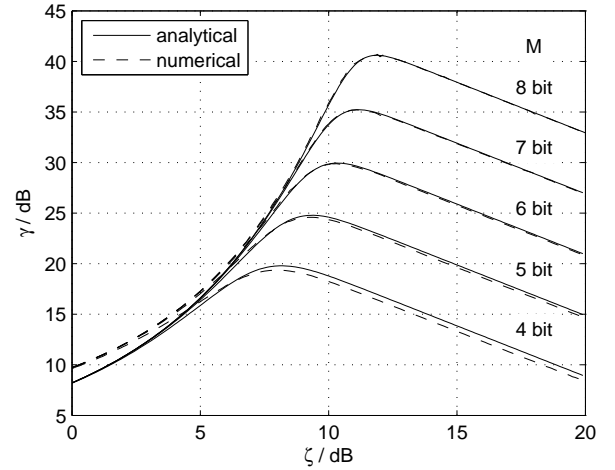


**Figure 2** SNR after clipping and quantization as a function of clipping ratio for different converter resolutions.

a comparison of simulation and analytical results for different  $M$ . It can be seen that the analytical and numerical results are in very good agreement, differences occur only for low values of  $\gamma$  caused by the blind SNR estimation algorithm used in the simulations. For each  $M$  there is a distinct maximum at a certain clipping ratio  $\zeta_{\text{opt}}$ , where for  $\zeta < \zeta_{\text{opt}}$  clipping noise dominates and for  $\zeta > \zeta_{\text{opt}}$  quantization noise dominates. In Section 3 we will study the impact of clipping and

quantization on the system performance and present a method to adjust quantization and clipping in such a way that system performance is high while keeping hardware complexity low.

### 3 Impact of requantization and re-quantization methods

To study the impact of requantization on the system performance we use the system model shown in Fig. 1. In this section we assume an ideal ADC without quantization at the receiver side. The influence of the ADC is shown later in Section 4. In our simulations, we vary the DAC resolution  $M$ , consider various modulation orders such as 4-, 16- and 64-QAM and compute the bit error rate (BER) as a function of the optical signal-to-noise ratio (OSNR). We compare the results with an ideal DAC, i.e. without quantization and clipping. The results can be seen in Fig. 3 for a DAC resolution of 5 bit. The OSNR penalty at a BER of  $10^{-3}$  is only 0.2 dB for 4-QAM and 0.6 dB for 16-QAM. However, for 64-QAM the loss is 3.7 dB. In Fig. 4 a comparison

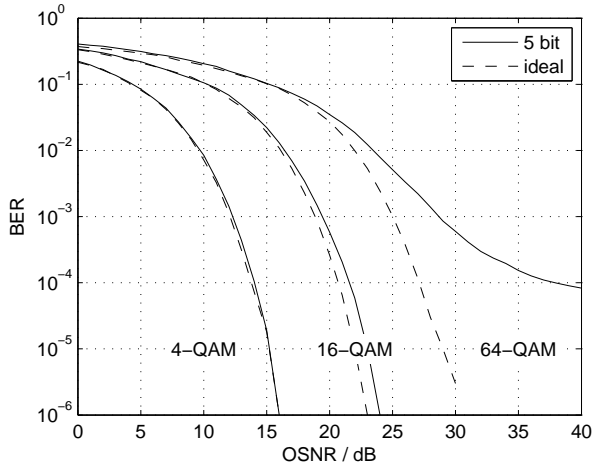


Figure 3 Impact of requantization using optimal clipping ratio compared to ideal model. DAC resolution 5 bit.

between different DAC resolutions using 64-QAM as modulation order is shown. A resolution of 4 bit cannot achieve a BER of  $10^{-3}$ . Using a resolution of 6 bit instead of 5 bit, the required OSNR for a BER of  $10^{-3}$  decreases by 2.4 dB. However, higher resolutions than 6 bit do not improve the system performance significantly.

#### 3.1 Shift and clip (SAC) method for re-quantization

Requantization with optimal clipping ratio normally requires a high hardware complexity. We present a method called SAC requantization which has reasonable hardware complexity at nearly the same system performance. The method is illustrated in Fig. 5. To

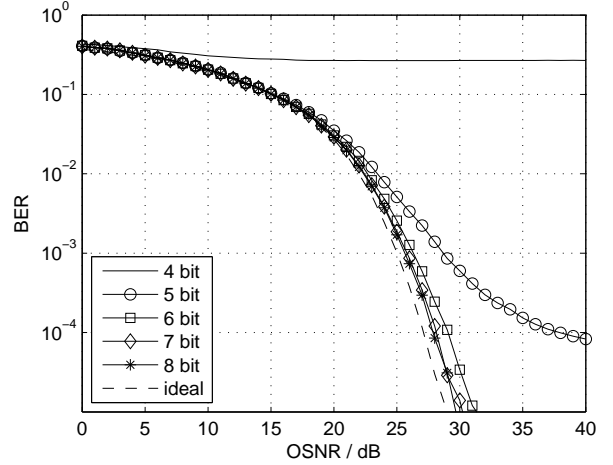


Figure 4 Impact of requantization using optimal clipping ratio compared to ideal model. DAC resolution from 4 bit to 8 bit and modulation 64-QAM.

show the principle we assume unsigned data. The first block represents the output signal of the IFFT. Least significant bit (LSB) and most significant bit (MSB) are located at the right and left side, respectively. Let us assume a word length of 9 bit. First, a right shift is executed. That means several LSBs are neglected, here 3 bit. Afterwards, we consider the MSBs, here 2 bit. If at least one MSB is unequal to zero, bits  $a_3, \dots, a_6$  are set to one, i.e. the output signal is set to the maximum value. Otherwise,  $a_3, \dots, a_6$  are left unchanged. This second step can be seen as an amplitude limitation and corresponds to the clipping of the OFDM signal.

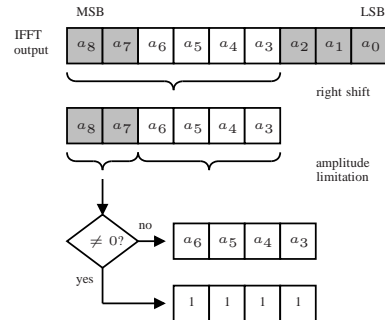
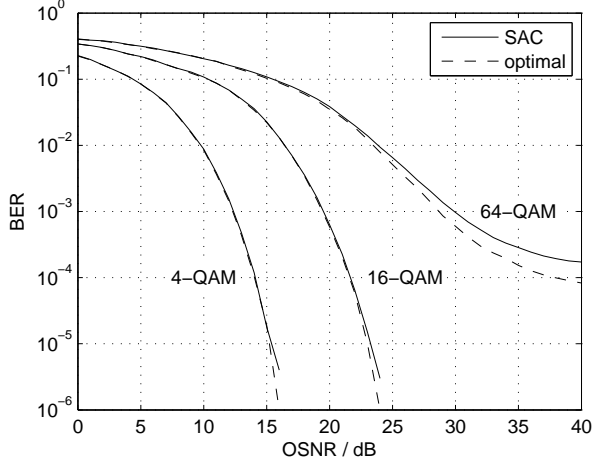


Figure 5 SAC requantizer. Example of requantization from 9 to 4 bit.

#### 3.2 Comparison of SAC with optimal clipping

To compare the performance of the SAC method with optimal clipping we compute the BER of the whole system including fiber for 4-, 16- and 64-QAM using a DAC resolution of 5 bit. The result is shown in Fig. 6. The OSNR penalty at a BER of  $10^{-3}$  is negligible for 4- and 16-QAM (0.06 dB and 0.09 dB, respectively). For 64-QAM the penalty increases to 1.22 dB. The reason why the OSNR difference between the SAC method and optimal clipping is small can be seen in more detail



**Figure 6** Comparison of SAC method and optimal clipping at DAC resolution 5 bit.

from **Fig. 7**. It shows the SNR at transmitter side  $\gamma_{TX}$  as a function of  $\zeta$  for 4-QAM and a DAC resolution of 5 bit (dashed line). When using the SAC method the maximum SNR generally cannot be achieved because the clipping ratio can only have discrete values (solid line with markers). **Fig. 7** also shows the required OSNR for a BER of  $10^{-3}$  as a function of  $\zeta$ . This curve is flat in a large region of  $\zeta$ . Consequently, the non-optimal choice of clipping ratio due to the SAC method has little impact on the system performance.

We want to derive an expression for the SNR at receiver side  $\gamma_{RX}$  and assume that the mean signal power  $\bar{P}$  of the received signal after amplification is equal to the mean transmitted signal power. At transmitter side

$$\gamma_{TX} = 10 \log_{10} \frac{\bar{P}}{N_{TX}} \quad (8)$$

with  $N_{TX} = N_q + N_{clip}$ . Furthermore,

$$\gamma_{RX} = 10 \log_{10} \frac{\bar{P}}{N_{TX} + N_{Ch}}, \quad (9)$$

where  $N_{Ch}$  is the mean noise power of the optical link. Using the definition of OSNR

$$\text{OSNR} = 10 \log_{10} \frac{\bar{P}}{\frac{12.5 \text{ GHz}}{B} N_{Ch}}, \quad (10)$$

where  $B$  is the signal bandwidth, we rewrite (9) with (8):

$$\gamma_{RX} = 10 \log_{10} \frac{1}{10^{-\gamma_{TX}/10} + \frac{B}{12.5 \text{ GHz}} 10^{-\text{OSNR}/10}}. \quad (11)$$

Taking typical values for sampling frequency  $f_A = 32 \text{ GHz}$ , number of subcarriers  $N = 256$ , number of zero padded subcarriers  $N_{ZP} = 91$ , OSNR = 12 dB and  $\gamma_{TX} = 30 \text{ dB}$  the resulting SNR on receiver side with  $B \approx f_A \frac{N - N_{ZP}}{N}$  is  $\gamma_{RX} = 9.78 \text{ dB}$  and with  $\gamma_{TX} = 25 \text{ dB}$  is  $\gamma_{RX} = 9.70 \text{ dB}$ . A SNR decrease by 5 dB at transmitter side thus only leads to a SNR

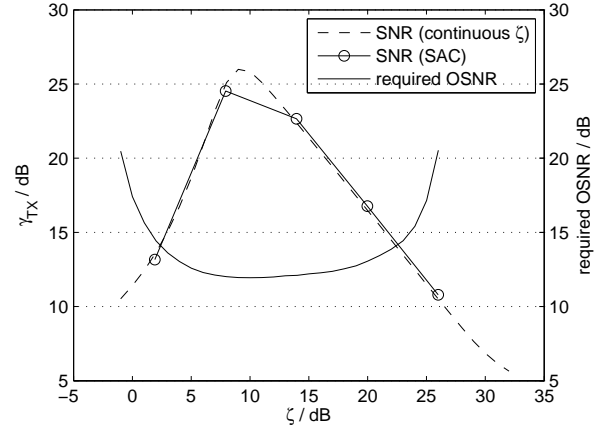


**Figure 7** Required OSNR for BER  $10^{-3}$  for 4-QAM and DAC resolution 5 bit and SNR at transmitter side.

decrease of 0.08 dB at receiver side in this example, because channel noise dominates.

In **Fig. 8** the required OSNR for a BER of  $10^{-3}$  for different DAC resolutions and modulation orders is shown. The 4-QAM turns out to be insensitive to clipping for a large range of  $\zeta$ . Sensitivity increases with decreasing DAC resolution and increasing modulation order. For 64-QAM and DAC resolutions greater than or equal to 7 bit, the system is still insensitive to clipping in a relatively wide range of  $\zeta$ . However, for DAC resolutions of 5 and 6 bit at 64-QAM, the required OSNR is strongly dependent on the clipping ratio  $\zeta$ . With a DAC resolution of 4 bit a BER of  $10^{-3}$  can't be reached for 64-QAM.

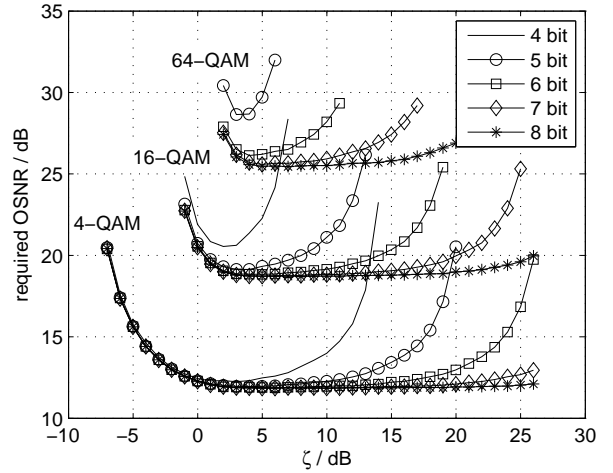


**Figure 8** Required OSNR for BER  $10^{-3}$  as a function of clipping ratio  $\zeta$  for different DAC resolutions and modulation orders.

## 4 Impact of ADC resolution

In the previous simulations, no quantization by the ADC was considered. Now we also study the impact of ADC resolution on the system performance. In **Fig. 9**

the required OSNR for BER  $10^{-3}$  is shown for 4-, 16- and 64-QAM. The DAC as well as the ADC resolutions range from 4 bit to 8 bit. For 4-QAM the required

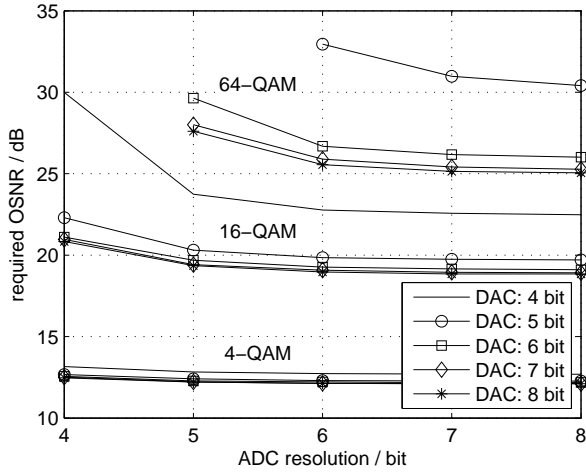


**Figure 9** Required OSNR for BER  $10^{-3}$  for 4-, 16- and 64-QAM at different DAC and ADC resolutions.

OSNR is nearly independent of the DAC and ADC resolutions. With 64-QAM and an ADC resolution greater than or equal to 6 bit the required OSNR is still almost constant except for DAC resolution 5 bit. With an ADC resolution of 6 bit and 64-QAM the OSNR penalty between DAC resolution 5 bit and 6 bit is 6.3 dB and thus quite significant. Reducing the ADC resolution from 6 bit to 5 bit with a 6-bit-DAC results in an OSNR loss of only 2.9 dB. This means the impact of the DAC is much stronger than that of the ADC.

## 5 Impact of requantization on channel estimation

So far we have assumed that the channel parameters are known in the receiver enabling perfect equalization of the received signal. However, for a realistic model, noise from the optical link and also quantization noise have to be considered for channel estimation. In this section we first study data-aided channel estimation. We assume that amplified spontaneous emission (ASE) noise of an EDFA at the receiver is turned into electrical additive white Gaussian noise (AWGN) after coherent optical demodulation. Further, we will introduce and evaluate two methods to mitigate the influence of quantization noise on channel estimation.

### 5.1 Channel estimation

For channel estimation, we consider a data-aided procedure that consists of periodically transmitted OFDM pilot symbols which are known in the receiver. Pilot symbols are defined in frequency domain where each subcarrier  $\nu$  is modulated with a known complex 4-QAM symbol  $X_\nu$ . We assume that chromatic dispersion is compensated completely by insertion of a guard

interval and the model of the time-invariant channel is expressed by

$$Y_{\nu,k} = H_\nu X_{\nu,k} + n_{\nu,k} \quad (12)$$

where  $X_{\nu,k}$  and  $Y_{\nu,k}$  are the transmitted and received  $k$ th OFDM symbols ( $k = 1, \dots, N_p$ ) respectively,  $H_\nu$  is the channel coefficient at frequency index  $\nu$  and  $n_{\nu,k}$  is zero-mean additive white Gaussian noise of the channel. For known and equal pilot symbols  $X_{\nu,k} = X_\nu$  the estimated channel coefficients  $\hat{H}_\nu$  are calculated by

$$\hat{H}_\nu = \frac{1}{N_p} \sum_{k=1}^{N_p} \frac{Y_{\nu,k}}{X_\nu} = H_\nu + \frac{1}{X_\nu} \left( \frac{1}{N_p} \sum_{k=1}^{N_p} n_{\nu,k} \right). \quad (13)$$

In (13) the second addend in brackets approaches the expected value  $E[n_{\nu,k}]$  with  $E[n_{\nu,k}] = 0$  for  $N_p \rightarrow \infty$ , thus reducing the noise impact on the channel estimation for large  $N_p$ . **Fig. 10** shows the BER as a function of OSNR and a comparison of the estimated channel with the ideally known channel for  $N_p = 10$  and different modulation orders. When neglecting quantization effects this estimation yields small OSNR penalties of around 0.4 dB at a BER of  $10^{-3}$ .

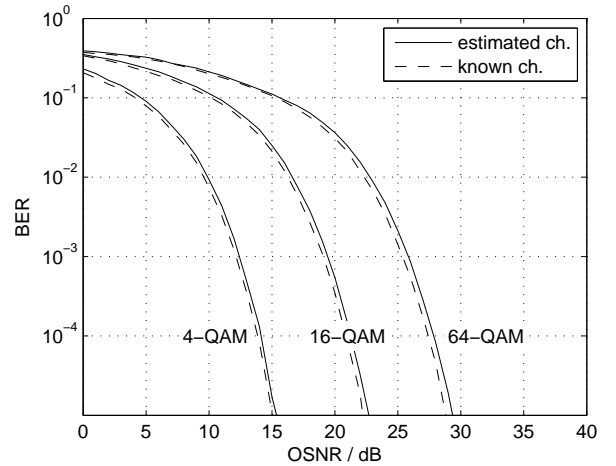


**Figure 10** Simulated BER for estimated and known channel for  $N_p = 10$ , no quantization effects.

### 5.2 Impact of quantization noise

We now consider limited DAC resolution and  $X_{\nu,k} = X_\nu$  ( $k = 1, \dots, N_p$ ) by adding quantization and clipping noise  $n_\nu^q$  to the transmitted pilot symbol. Impact of the ADC is neglected here. Then (12) becomes

$$Y_{\nu,k} = H_\nu (X_\nu + n_\nu^q) + n_{\nu,k} \quad (14)$$

and the channel estimation in (13) is extended to

$$\begin{aligned}\hat{H}_\nu &= \frac{1}{N_p} \sum_{k=1}^{N_p} \left[ H_\nu + \frac{H_\nu}{X_\nu} n_\nu^q + \frac{n_{\nu,k}}{X_\nu} \right] \\ &= H_\nu + \frac{H_\nu}{X_\nu} n_\nu^q + \frac{1}{N_p X_\nu} \sum_{k=1}^{N_p} n_{\nu,k}.\end{aligned}\quad (15)$$

It can be seen from the above formulation that the second addend introduces an additional noise component that cannot be averaged out over  $N_p$  pilots. An example for the impact of this additional noise component on the BER is given in **Fig. 11** (circle markers). In the following Sections 5.3 and 5.4 we will present two methods to mitigate the influence of quantization on channel estimation.

### 5.3 Channel estimation using different pilot symbols

A straight-forward approach to solve the problem stated in section 5.2 is to transmit  $N_p$  different pilot symbols  $X_{\nu,k}$ . The idea behind this method is to introduce a random variation to  $n_\nu^q$  that enables mitigation of the quantization noise component by calculating the mean as it is done anyway in (13) to improve channel estimation. Introduction of different pilot symbols finally yields

$$\hat{H}_\nu = H_\nu + \frac{H_\nu}{N_p} \sum_{k=1}^{N_p} \frac{n_{\nu,k}^q}{X_{\nu,k}} + \frac{1}{N_p} \sum_{k=1}^{N_p} \frac{n_{\nu,k}}{X_{\nu,k}}.\quad (16)$$

Considering the expected value of  $\hat{H}_\nu$ , we find that the third term in (16) approaches zero for  $N_p \rightarrow \infty$ , because  $n_{\nu,k}$  and  $X_{\nu,k}$  are statistically independent and  $n_{\nu,k}$  has zero mean. The second term also approaches zero if  $X_{\nu,k}$  and  $n_\nu^q$  are uncorrelated which is mostly the case, as shown in [12]. Fig. 11 shows the effectiveness of the method taking the example of a DAC resolution of 5 bit. While a repetition of the same pilot symbol introduces significant OSNR penalties and even renders transmission with a BER of  $10^{-3}$  impossible for 64-QAM, the method with different pilot symbols (solid line) can nearly remove the impact of quantization. Yet, for 64-QAM an OSNR penalty of 1.7 dB compared to the known channel remains. In section 5.4 we will investigate how this penalty can be further reduced.

### 5.4 Quantization aware channel estimation

As pointed out in Section 5.2, actually the time domain versions of the quantized pilot symbols  $X_\nu^q = X_\nu + n_\nu^q$  are transmitted as given in (14). Consequently,  $X_\nu^q$  has to be provided to the receiver rather than  $X_\nu$ . As a result, the estimation yields

$$\hat{H}_\nu = \frac{1}{N_p} \sum_{k=1}^{N_p} \frac{Y_{\nu,k}}{X_\nu^q} = H_\nu + \frac{1}{X_\nu^q} \left( \frac{1}{N_p} \sum_{k=1}^{N_p} n_{\nu,k} \right).\quad (17)$$

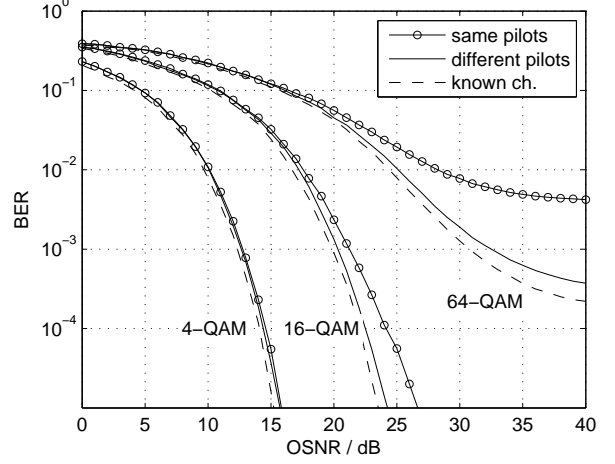


**Figure 11** Simulated BER at DAC resolution 5 bit for two channel estimation methods compared to known channel.

$X_\nu^q$  can be calculated by the scheme depicted in **Fig. 12** that uses an FFT operation to transform the quantized time domain pilot symbols back to frequency domain to obtain the pilot symbol  $X_\nu^q$ .

In a practical implementation there is no need to actually integrate an additional FFT block into the transmitter, because  $X_\nu^q$  can be calculated offline once. Pilot symbols will generally be fixed in the

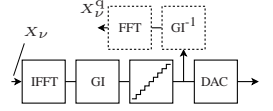


**Figure 12** Proposed scheme for calculation of pilot symbols  $X_\nu^q$ .

system development phase and will not be changed later or dynamically. In this case the scheme proposed here does not add any additional complexity to transmitter or receiver. In **Fig. 13** all proposed channel estimation schemes are compared by means of the required OSNR for a BER of  $10^{-3}$ . Significant differences are mainly

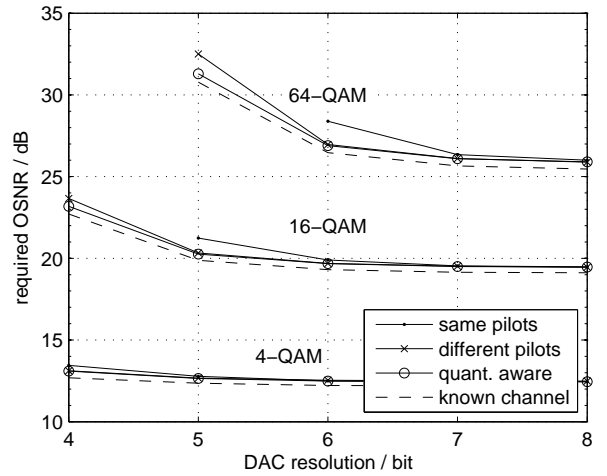


**Figure 13** Required OSNR for  $\text{BER} = 10^{-3}$  for different channel estimation schemes as a function of DAC resolution.  $N_p = 10$ .

observed for high modulation orders (16- and 64-QAM)

and low DAC resolutions ( $< 7$  bit). The quantization aware estimation scheme achieves the lowest required OSNR in all cases. **Tab. 1** points out the differences between the estimation results for 64-QAM by providing the difference of the required OSNR for a BER of  $10^{-3}$  for the known channel and the respective channel estimation scheme. While having little effect for DAC

M / bit	5	6	7	8
same pilots	-	1.93	0.69	0.54
different pilots	1.72	0.50	0.45	0.42
quantization aware	0.51	0.43	0.45	0.44

**Table 1** OSNR penalties in dB with respect to known channel at BER =  $10^{-3}$ , 64-QAM

resolutions greater than or equal to 7 bit, the choice of the channel estimation scheme becomes important for the more realistic resolutions of 5 and 6 bit. It is also observed that the quantization aware estimation scheme yields the same penalty as channel estimation in the case of no quantization. These simulation results and eq. (17) show that the proposed method effectively removes the impact of clipping and quantization on channel estimation.

## 6 Conclusion

In this paper we provided the optimal clipping ratio for DAC resolutions 4 to 8 bit and showed that O-OFDM transmission achieving a BER of  $10^{-3}$  is possible with modulation orders of up to 64-QAM using DAC and ADC resolutions as low as 6 bit at sampling frequency 32 GSa/s resulting in data rates of up to 240 Gbit/s. With the SAC method we presented a clipping method that reduces hardware complexity while introducing only negligible OSNR penalties. Furthermore, we introduced a quantization aware channel estimation method that achieves an OSNR gain of up to 1.5 dB compared to existing methods while keeping hardware complexity low.

## 7 Acknowledgment

This work was carried out in the framework of DFG project “Elektronische Schlüsselbausteine für optische OFDM-Systeme hoher Bitrate”. The support of DFG is gratefully acknowledged.

## References

- [1] F. Buchali, R. Dischler, A. Klekamp, M. Bernhard, and D. Efinger, “Realisation of a real-time 12.1 Gb/s optical OFDM transmitter and its application in a 109 Gb/s transmission system with coherent reception,” in *Optical Communication, 2009. ECOC '09. 35th European Conference on*, vol. 2009-Supplement, Sept. 2009, pp. 1–2.
- [2] F. Buchali, X. Xiao, S. Chen, and M. Bernhard, “Towards real-time CO-OFDM transceivers,” in *Optical Fiber Communication Conference and Exposition (OFC/NFOEC), 2011 and the National Fiber Optic Engineers Conference*, March 2011, pp. 1–4.

- [3] R. Giddings, X. Jin, E. Hugues-Salas, E. Giacomidis, and J. Tang, “Experimental demonstration of record high 11.25Gb/s real-time end-to-end optical OFDM transceivers for PONs,” in *Future Network and Mobile Summit, 2010*, June 2010, pp. 1–13.
- [4] B. Inan, O. Karakaya, P. Kainzmaier, S. Adhikari, S. Calabro, V. Sleiffer, N. Hanik, and S. Jansen, “Realization of a 23.9 Gb/s real time optical-OFDM transmitter with a 1024 point IFFT,” in *Optical Fiber Communication Conference and Exposition (OFC/NFOEC), 2011 and the National Fiber Optic Engineers Conference*, March 2011, pp. 1–3.
- [5] R. Bouziane, P. Milder, R. Koutsoyannis, Y. Benlachtar, C. Berger, J. Hoe, M. Püschel, M. Glick, and R. Killey, “Design studies for an ASIC implementation of an optical OFDM transceiver,” in *Optical Communication (ECOC), 2010 36th European Conference and Exhibition on*, Sept. 2010, pp. 1–3.
- [6] S. Wei, D. Goeckel, and P. Kelly, “Convergence of the complex envelope of bandlimited OFDM signals,” *Information Theory, IEEE Transactions on*, vol. 56, no. 10, pp. 4893–4904, 2010.
- [7] B. Murmann, “ADC Performance Survey 1997-2011,” 2011. [Online]. Available: <http://www.stanford.edu/~murmann/adcsurvey.html>
- [8] T. Alpert, F. Lang, and D. Ferenci, “A 28GS/s 6b pseudo segmented current steering DAC in 90nm CMOS,” *Microwave Symposium Digest (MTT), 2011 IEEE MTT-S International*, pp. 6–9, 2011.
- [9] Y. Greshishchev, D. Pollex, S. Wang, M. Besson, P. Flemeke, S. Szilagyi, J. Aguirre, C. Falt, N. Ben-Hamida, R. Gibbins, and Others, “A 56GS/s 6b DAC in 65nm CMOS with 256x6b memory,” in *Solid-State Circuits Conference Digest of Technical Papers (ISSCC), 2011 IEEE International*, vol. 21, no. 1. IEEE, 2011, pp. 194–196.
- [10] D. Mestdagh, P. Spruyt, and B. Biran, “Analysis of clipping effect in DMT-based ADSL systems,” in *Communications, 1994. ICC'94, SUPERCOMM/ICC'94, Conference Record, Serving Humanity Through Communications. IEEE International Conference on*. IEEE, 1994, pp. 293–300.
- [11] H. Ehm, S. Winter, and R. Weigel, “Analytic quantization modeling of OFDM signals using normal Gaussian distribution,” in *Microwave Conference, 2006. APMC 2006. Asia-Pacific*, vol. 2. IEEE, 2006, pp. 847–850.
- [12] A. Sripad and D. L. Snyder, “A Necessary and Sufficient Condition for Quantization Errors to be Uniform and White,” *IEEE Transactions on Acoustics, Speech and Signal Processing*, no. 5, pp. 442–448, 1977.